Sukhomlinov, Dmitry; Virtanen, Olli; Latostenmaa, Petri; Jokilaakso, Ari; Taskinen, Pekka

Impact of MgO and K_2O on Slag-Nickel Matte Equilibria

Published in:
Journal of Phase Equilibria and Diffusion

DOI:
10.1007/s11669-019-00767-3

Published: 01/12/2019

Document Version
Publisher's PDF, also known as Version of record

J. Phase Equilib. Diffus. (2019) 40:768–778
https://doi.org/10.1007/s11669-019-00767-3

Impact of MgO and K_2O on Slag-Nickel Matte Equilibria

Dmitry Sukhomlinov[1,2] · Olli Virtanen[1] · Petri Latostenmaa[3] · Ari Jokilaakso[1] · Pekka Taskinen[1]

Submitted: 30 August 2019 / in revised form: 23 October 2019 / Published online: 13 November 2019

Abstract Slag chemistry of the direct nickel matte smelting was studied in typical industrial high-grade nickel matte smelting conditions at 1400 °C and 0.1 atm p_{SO2}. The experimental technique used involved equilibration, quenching and direct elemental phase composition analysis by Electron Probe X-ray Microanalysis. Magnesia and potassia, a typical gangue constituent of sulfidic nickel concentrates and a common impurity of industrial grade silica flux (sand), respectively, were adopted as slag modifiers in concentrations typical to industrial operations. Their effects on oxidation degree of the nickel-copper-iron matte and equilibrium concentrations of Ni and Cu in the slag were studied as a function of oxygen partial pressure. Solubility of silica in the slag increased significantly with additions of MgO and K_2O in the constrained case studied, at silica saturation. Equilibrium concentrations of Ni and Cu in the slag containing MgO and K_2O were about a quarter lower compared to the pure iron silicate slag, in the entire oxygen partial pressure range studied.

Keywords flash smelting · fluxing · phase equilibria · thermodynamics

1 Introduction

A quarter-century ago the DON (Direct Outotec Nickel) smelting technology was first time industrially implemented at Harjavalta (Finland), replacing the conventional sulfide nickel concentrate smelting- matte converting route. In this converter-less nickel matte smelting technology, a FSF (flash smelting furnace) produces high grade nickel matte with a low iron concentration, while an EF (electric furnace) is employed to recover the metal values from the smelting slag to iron-rich matte (alloy). By introducing this technology at Harjavalta, the production throughput grew three-fold. Meanwhile, the environmental impact was decreased due to elimination of the converting step and production of strong sulfur dioxide off-gas in the flash smelting furnace, which was then fully collected and converted to sulfuric acid.[1,2]

Conventional sulfidic nickel bulk concentrates have a wide compositional range. Usual concentration of nickel varies from 5 to 12 wt.%, while concentration of copper ranges from 1 to 6 wt.%. Trends of decreasing valuable metal contents[3] as well as decreasing Ni/Cu ratio in the available concentrates have been reported. In addition, PGMs (platinum group metals) and cobalt are valuable trace constituents of sulfidic nickel concentrates. The concentration of the latter can range from 0.2 to 1 wt.%.[4] Typical low grade sulfidic nickel concentrates contain significant fractions of MgO in the gangue, while technical grade silica flux utilized by smelters often contains some K_2O as a constituent of its trace minerals, such as feldspar

Electronic supplementary material The online version of this article (https://doi.org/10.1007/s11669-019-00767-3) contains supplementary material, which is available to authorized users.

✉ Pekka Taskinen
pekka.taskinen@aalto.fi

[1] Department of Chemical and Metallurgical Engineering, Aalto University, PO Box 16100, 00076 Aalto, Finland

[2] Present Address: Department of Materials Science and Engineering, Norwegian University of Science and Technology, 7034 Trondheim, Norway

[3] Boliden Harjavalta, Teollisuuskatu 1, 29200 Harjavalta, Finland

and mica. The DON smelting technology was developed for processing sulfidic, high magnesia nickel concentrates, and showed robustness also in the processing bulk concentrates with various Ni/Cu ratios, while providing high recovery of nickel and copper, as well as PGMs and cobalt.[4–6]

1.1 Features of DON Smelting Technology

The DON smelting technology was developed by Outokumpu in early 1990s and launched in Harjavalta, Finland (1995) and later in Fortaleza, Brazil (1998).[4] This technology can cope with processing of complex and low grade concentrates with variable copper-to-nickel ratios. It comprises a few stages, i.e. smelting of dried sulfidic concentrates along with silica flux in a FSF and a subsequent hydrometallurgical processing of granulated iron-lean matte to metal. The metal value from FSF slag is recovered in an EF by coke reduction. Thus, two different matte grades and types are produced by the DON technology. The de-dusted off-gas from FSF is sent to sulfuric acid plant, while the captured dust is recirculated back to the FSF. Therefore, one of the technological advantages is a lower cost of the off-gas treatment and higher efficiency of SO_2 capturing.[7] Absence of converters in the processing line and as a consequence a lower CAPEX are the key benefits,[2] compared to the conventional sulfidic nickel smelting-converting routes. High resource efficiency due to absence of the internally circulating slag is a great promoter of this process in the future. An update of the technology was recently given by Johto et al.[6]

The unusual feature of this technology is production of an iron-lean sulfide matte, typically with less than 10 wt.% Fe, and a larger slag volume compared to the conventional matte smelting. In the DON smelting process, the feed mixture is subjected to more extended iron oxidation,[8] which facilitates fluxing of MgO more efficiently compared to the conventional nickel smelting end-point.[6] Magnesia increases viscosity and liquidus temperature of the iron silicate slag, while the higher degree of oxidation of iron and its diluting effect compensates it and allows operation of the smelting process at a lower temperature, when using the same Fe/MgO ratio in the feed mixture.

1.2 Previous Studies

The phase equilibrium data and thermodynamics of nickel-iron matte converting conditions were reviewed by Kellogg.[9] Font et al.[10–12] and Henao et al.[13] investigated experimentally phase equilibria between nickel mattes and MgO-saturated iron silicate slags in controlled gas atmospheres. Henao et al.[14] studied nickel distributions in copper-free mattes using various slag chemistries. Taskinen et al.[15] measured oxygen activities and chemical analysis data of the phases during the industrial operations of a nickel FSF and a slag-cleaning EF. In addition, the mechanisms of slag and matte formation and minor elements partitioning in the industrial DON process were reported. Mäkinen and Taskinen[1] investigated the liquidus in MgO-containing iron silicate slags as a function of temperature and Fe/SiO_2 ratio. Strengell et al.[16] investigated effect of MgO concentration in iron silicate slag on nickel and copper solubilities in the slag as a function of iron content in nickel-copper-iron matte from 1523 to 1723 K (1350 to 1450 °C) in 0.1 atm p_{SO2}.

The deportment of trace elements between nickel-copper-iron matte and iron silicate slag was investigated experimentally by Font et al.[11] Recently, fundamentals of trace element partitioning in the DON smelting conditions, including operation conditions of FSF[17,18] and EF[19,20] have been investigated experimentally.

1.3 The Current Objectives

The present experimental study was focused on the investigation of the high-grade nickel matte smelting slag chemistry and on the effects of MgO and K_2O on slag and matte compositions at different end-points of the smelting. To increase the basic knowledge, the laboratory equilibration experiments were conducted in the DON smelting process conditions. The trace element distributions measured along with the slag and matte properties have recently been reported elsewhere.[18]

2 Experimental

This study employed an experimental technique, which combines high-temperature equilibration with rapid quenching and direct analysis of the phase compositions in the samples post quenching. The isothermal equilibration of nickel-copper-iron matte with silica-saturated iron silicate slag was conducted in controlled, flowing gas atmospheres at 1673 K (1400 °C). The gas mixture comprised of SO_2, CO, CO_2, and Ar. Magnesium and potassium oxides were utilized as slag modifiers. The prevailing oxygen partial pressure and concentrations of the slag modifiers (MgO and K_2O) varied in the experimental set. The experimental technique used for nickel-copper-iron matte equilibration with slag in a controlled gas atmosphere has been described in detail previously.[16,18]

2.1 Sample Preparation

The starting chemicals utilized in the study and their purities are summarized in Table 1. The experimental

Table 1 Purities and suppliers of the chemicals utilized in the experiments

Chemical	Supplier	Purity wt.%	Form
SiO_2	Umicore	99.99	Granulate
Fe_2O_3	Alfa Aesar	99.99	Powder
MgO	Sigma-Aldrich	99.995	Powder
K_2CO_3	Sigma-Aldrich	99.5–100.5	Powder
Ni_3S_2	Alfa Aesar	99.9	Powder
Cu_2S	Alfa Aesar	99.5	Powder
FeS	Alfa Aesar	99.9	Powder
Chemical	Supplier	Purity vol.%	Form
SO_2	Aga-Linde	99.98	Gas
CO	Aga-Linde	99.97	Gas
CO_2	Aga-Linde	99.9993	Gas
Ar	Aga-Linde	99.999	Gas

series consisted of equilibration experiments at 1673 K (1400 °C) for gas-matte-slag samples in small (10 mm outer diameter, 6 mm height) bowl-shaped, open fused silica crucibles (Finnish Special Glass, Espoo).

The studied sulfide mattes and slags were synthetized from pure sulfide and oxide powders. The mass of their initial powder mixture was about 0.1 g. The target ratio of Ni to Cu concentrations in matte was 5 to 1 (w/w). In this regard, pure sulfides of nickel and copper were mixed with an appropriate ratio. The prevailing sulfur and oxygen pressures as two independent system variables defined the distribution of iron between the matte and the slag, based on the overall reaction:

$$\{FeS\}_{(matte)} + 1/2O_2(g) = [FeO]_{(slag)} + 1/2S_2(g) \qquad \text{(Eq 1)}$$

taking place during equilibration in the Ar-S_2-O_2-SO_2 atmosphere in flowing CO-CO_2-SO_2-Ar mixtures which fix the oxygen and sulfur partial pressures in the furnace and thus post equilibration in the sample.

Weight fractions of Fe_2O_3 and SiO_2 in the starting powder mixture were equal, while pre-calculated fractions of magnesia (10 wt.% MgO) or/and potassium oxide (2 wt.% K_2O) were added in selected samples as slag modifiers. Potassium oxide was introduced into the system as potassium silicate, which was synthesized beforehand from a mixture of pulverized silica and potassium carbonate, see Table 1. The mixture with a small excess of silica (referred to K_2SiO_3) was calcined at 1473 K (1200 °C) in a platinum crucible and then annealed at 873 K (600 °C) in a muffle furnace in air atmosphere.

2.2 High Temperature Experimental Setup

The isothermal conditions during the equilibrations were maintained with a Lenton PTF 15/45/450 resistance tube furnace (Lenton, UK). A gas-impermeable alumina tube Degussit AL23 (Friatec, Germany) was employed for the equilibrations as the furnace work tube with the following dimensions: 38 × 45 × 1100 mm (inner diameter/outer diameter/length). The total gas flow rate was 400 mL/min, while the individual flow rates of the pure gases, see Table 1, were pre-calculated beforehand and they were regulated with DFC26 digital mass-flow controllers (Aalborg, USA). The gases were pre-mixed at room temperature in an alumina pebble column before leading to the furnace. Sulfur dioxide partial pressure was fixed to 0.1 atm in all experiments, while volumetric fractions of CO and CO_2 varied depending on the target iron concentration in the sulfide matte, see Table 2. The partial pressures of oxygen and sulfur generated were calculated using the SGTE data for pure substances.[21]

The sample temperature was measured during the entire equilibration period by a calibrated S-type thermocouple Pt /90%Pt-10%Rh (Johnson-Matthey, UK), which was located right next to the sample in the work tube. The thermocouple was connected to a Keithley 2010 DMM multimeter (Keithley, USA), while a PT100 resistance thermometer (tolerance class B 1/10, SKS-Group, Finland) connected to a Keithley 2000 DMM multimeter measured the cold junction temperature. The uncertainty of the temperature measurements was estimated as ±3 K. The details of the experimental furnace and its gas train have been described in previous publications.[17,22]

In a preliminary time series of experimental runs, the time sufficient to attain equilibrium was determined to be four hours, as described earlier.[18] This equilibration time was employed for all experiments in the main series. The main series of equilibration experiments was completely duplicated to confirm repeatability of the results.

2.3 Sample Analysis Post Quenching

After equilibration, the samples were rapidly quenched in an ice-water mixture to retain their equilibrium phases and their compositions. Polished sections of the samples post quenching were prepared for EPMA (Electron Probe X-ray Microanalyzer) analysis by employing traditional metallographic wet methods of grinding and polishing. Elemental concentrations in each phase were analyzed with a Cameca SX-100 EPMA equipped with five wavelength dispersive spectrometers (Cameca SAS, France). A defocused 100 μm electron beam (20 to 50 μm in the slag phase of a few samples with smaller slag areas) was used for matte with an acceleration voltage of 20 kV and a beam

Table 2 Gas flow rates utilized for each target iron concentration in matte and corresponding equilibrium partial pressures of oxygen and sulfur at 1673 K (1400 °C)

Target Fe concentration in matte, wt.%	Flow rate, mL/min				Equilibrium $\log_{10}$, pO_2/atm	Equilibrium $\log_{10}$, pS_2/atm
	SO_2	CO	CO_2	Ar		
3	40	8.1	51.9	300	−6.8(3)	−3.3(3)
6	40	11.0	49.0	300	−7.0(3)	−2.9(3)
9	40	13.3	46.7	300	−7.1(5)	−2.7(2)
11	40	16.0	44.0	300	−7.2(5)	−2.5(4)

Table 3 Elemental detection limits for matte and slag phases in the present EPMA measurements

Detection limit, ppmw	O	Si	Mg	S	K	Fe	Cu	Ni
Matte	1500	95	170	140	50	180	395	275
Slag	1200	185	200	110	60	195	275	225

current of 60 nA. Eight spots were analyzed from each phase in every sample for statistical reliability. The employed external standards and X-ray lines analyzed were hematite (O Kα and Fe Kα), quartz (Si Kα), diopside (Mg Kα), sanidine (K Kα), pentlandite (S Kα), metallic copper (Cu Kα), and metallic nickel (Ni Kα). ZAF correction by Cameca was used for the primary data, based on the approach of Pouchou and Pichoir.[23] The elemental detection limits of the EPMA were collected in Table 3 for each phase.

The Ziebold method was used for estimating the detection limits.[24] The values reported in Table 3 are based on the used measuring time, number of counts and signal-to-noise ratio of the element.

3 Results and Discussion

The experimental series was composed of three matte grades, with the target values of 3, 6, and 9 wt.% Fe calculated for the pure iron silicate system, and four slag compositions, iron silicate, MgO-, K_2O-, and MgO & K_2O-containing slags equilibrated in the same p_{S2}-p_{O2}-p_{SO2} points of the gas mixture. For K_2O- and MgO-free slags a series at 11 wt.% Fe in the matte was also accomplished. The molten slag and sulfide matte phase domains post quenching showed homogeneous glassy or microcrystalline structures, see Fig. 1, allowing reliable elemental analysis of the phase compositions with EPMA. The analysis was performed with well-quenched areas employing the significant spot size in the matte in order to further increase the reliability of the measurements. The experimental compositions and their standard deviations are also available in numerical form in the Supplementary Material.

3.1 Matte Composition

The average ratio of Ni to Cu concentrations in the sulfide matte measured for all experiments was 5.2 ± 0.3 (w/w) within the whole range of iron concentrations studied, see Fig. 2. The error bars in Fig. 2 were obtained from standard deviations of the EPMA measurements, as describer earlier.[16] The experimental uncertainties (1σ) in the sulfide matte are shown as error bars of the iron concentrations.

The measured iron concentration in matte controlled by the gas atmosphere varied from 2 to 11 wt.% Fe if all slag compositions in this study were taken into account, see Fig. 3. The slag composition, i.e. the slag modifiers used, affected the equilibrium iron concentration in matte at fixed sulfur and oxygen activities, too. Thus, the iron concentration in matte was varying from a span of about 2 to 8.5 wt.% Fe, decreasing with increase in pO_2 and with additions of basic oxides in the system (MgO or/and K_2O).

Their effect on the iron concentration in matte was more prominent in the lower oxygen partial pressures, see Fig. 3, i.e. at high end of iron concentrations of the sulfide matte studied. This is a consequence of the shape of oxygen partial pressure versus iron concentration behavior of the sulfide matte in the present conditions. The effect of magnesia on the equilibrium iron concentration in matte was significant, e.g. with 8.6 ± 0.3 wt.% MgO in the slag decreased iron concentration in the matte by 2 wt.% Fe at $\approx 10^{-7.1}$ atm oxygen partial pressure (approximately 7.5 wt.% [Fe] in matte in the MgO-free case), compared to the cases with pure iron silicate slag. On the other hand, the effect of potassium oxide with the concentration tested in this study (1.9 ± 0.2 wt.% K_2O) seemed to be very effective within the current domain of experiments, considering the small concentration range covered.

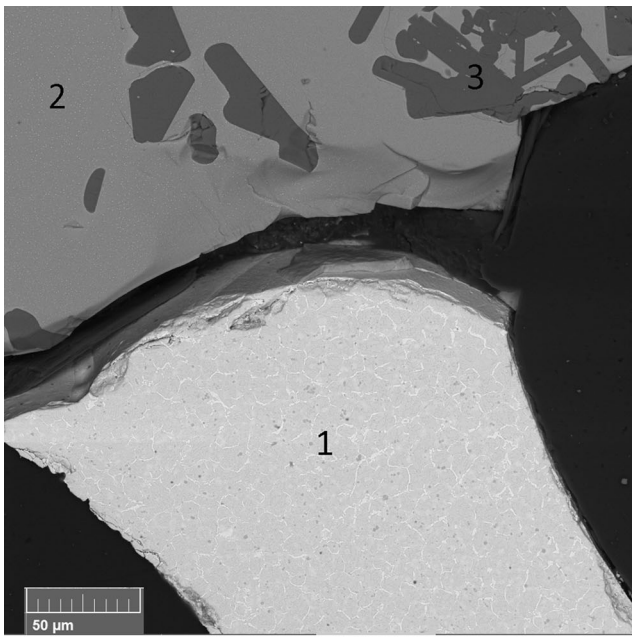

(a)

(b)

Fig. 1 Typical micrographs of a quenched slag-matte sample comprising of (1) sulfide matte, (2) slag, and (3) secondary tridymite crystals; 2 wt.% K_2O, equilibration at pO2 = 10–7.15 and pSO2 = 0.1 atm

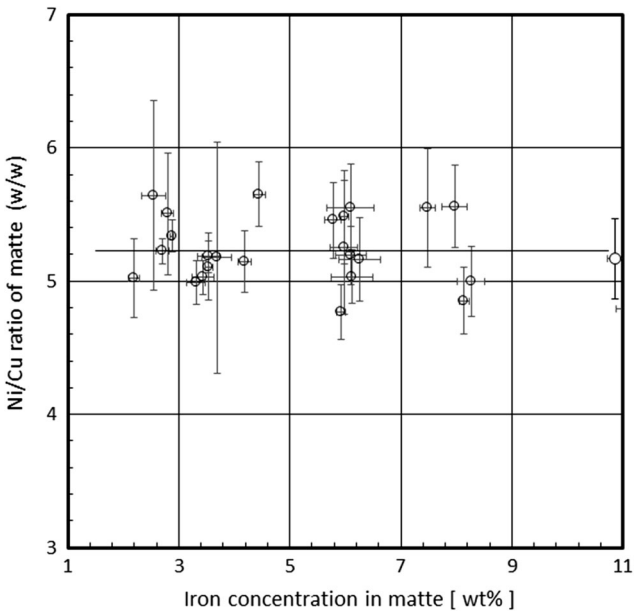

Fig. 2 The ratio of nickel to copper (w/w) in the nickel sulfide matte as a function of its iron concentration in the entire experimental series of this study

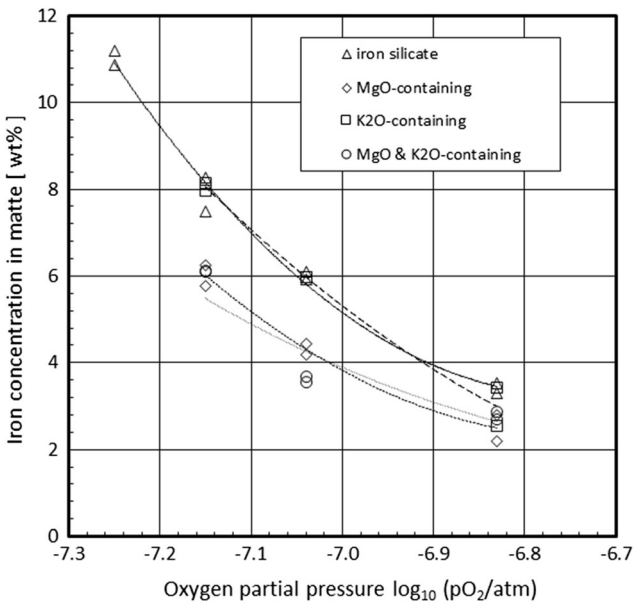

Fig. 3 Iron concentrations in the matte as a function of equilibrium oxygen partial pressure; the slag type was adopted as a parameter in the graph; MgO containing slags had 8.6 et% (MgO), K_2O containing 1.9 wt.% (K_2O), and MgO & K_2O containing 7.2 and 1.5 wt.%, respectively

Basic oxides adjust the activity coefficients of iron oxides in the silica saturated iron silicate slag and at a constant oxygen partial pressure they change the activity of iron in the equilibrium system, as shown earlier.[17] As a consequence, MgO and K_2O had a clear influence on the sulfide matte composition and particularly on the equilibrium concentration of iron in the nickel matte in each p_{O2}-p_{S2} point, see Fig. 3.

The concentrations of nickel and copper in matte increased with increasing oxygen partial pressure and decreasing iron concentration, while the ratio of their weight concentrations remained nearly constant, as stated

earlier. The ratio, thus, was essentially pre-defined by the composition of the starting mixture. On the other hand, the concentration of sulfur in the matte was slightly increasing with increasing concentration of iron in the matte, see Fig. 4, at constant sulfur dioxide partial pressure of 0.1 atm.

Figure 4 indicates clearly that when the matte assay was plotted as a function of iron concentration of the matte, no influence by the slag modifiers can be seen in the matte composition and they form a single line, independently of magnesia and potassia concentrations. A comparison with the sulfur concentrations of mattes with [Ni]/[Cu] = 4 by Piskunen et al.[17] show an excellent agreement with the present data.

3.2 Slag Composition

The solubility of silica in silica-saturated iron silicate slag, equilibrated at 1673 K (1400 °C) with the nickel-copper-iron matte, was approximately 37.4 wt.% SiO_2 (±0.3 wt.%) within the prevailing oxygen partial pressure range studied, showing no systematic influence of the iron concentration of matte. Additions of MgO and K_2O in the system substantially increased the solubility of silica. The former modifier (8.6 ± 0.3 wt.% MgO) alone increased the solubility of silica up to 45.0 wt.% SiO_2 (±0.8), while the latter one (1.9 ± 0.2 wt.% K_2O) increased it up to 46.6 wt.% SiO_2 (±0.9). Their cumulative effect (7.2 ± 0.3 wt.% MgO & 1.5 ± 0.1 wt.% K_2O) raised the solubility of silica to 50.4 wt.% (±1.1) SiO_2 and a minor decreasing trend could be observed along with increasing oxygen partial pressure.

These observations were valid for this constrained case where the liquid oxide (slag) was always saturated by silica, but in a relatively narrow oxygen partial pressure range of present study. The corresponding observations on the Fe/SiO_2 ratio (w/w) from 1.2 to 0.6 associated with additions of the basic oxides in the slag was plotted in Fig. 5, showing also the average value of the ratio for each slag type as a horizontal line.

The solubilities of nickel and copper in the slag equilibrated at 1673 K (1400 °C) with the nickel-copper-iron matte increased in oxidizing conditions. Addition of basic oxides MgO and K_2O in the slag decreased the equilibrium concentrations of Cu, Fe and Ni within the entire experimental range of oxygen partial pressure, see Fig. 6, compared to the simple case of ternary iron silicate slag of the system $FeO-Fe_2O_3-SiO_2$ at silica saturation. The MgO-free data by Piskunen et al.[17] (Ni/Cu = 4) are shown for comparison. The trend lines in Fig. 6 are based on the data of this study, only. The data by Font et al.[10–12] were available in graphical form only and, therefore, not used in the evaluations.

The concentration of sulfur in the studied slags increased along with iron concentration in the matte. It also was strongly reduced by additions of basic oxides in the slag, see Fig. 7, in a single p_{O2}-p_{S2} point. Their effect on the equilibrium concentration of sulfur in slags was prominent, i.e. sulfur concentration in the MgO & K_2O-

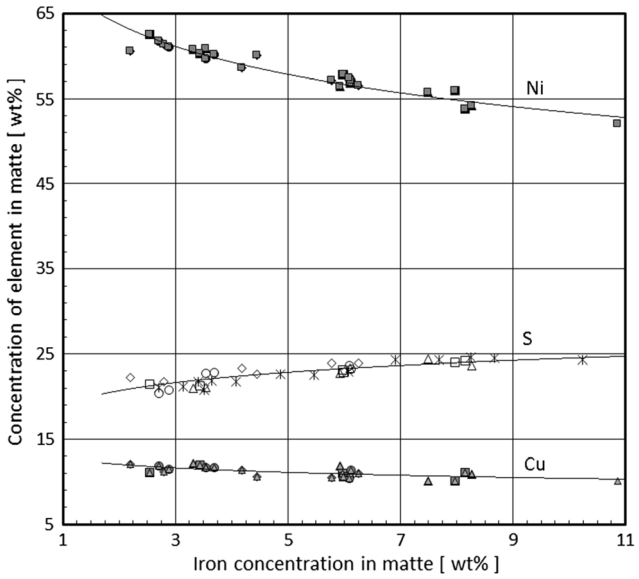

Fig. 4 Equilibrium concentrations of nickel (black), copper (grey), and sulfur (white) in matte as a function of its iron concentration; the symbols indicate the slag type as: triangle—iron silicate, diamond—MgO-containing, square—K_2O-containing, circle—MgO & K_2O-containing slag [* sulfur data by Piskunen et al.[17]]

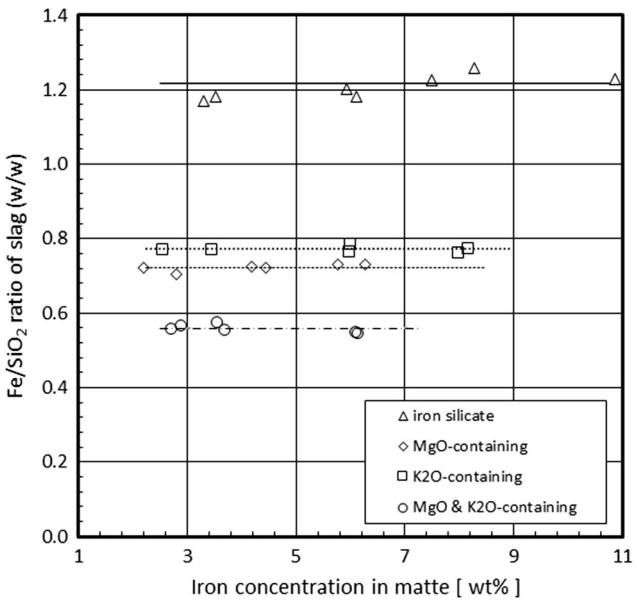

Fig. 5 The effect of slag modifiers (MgO and K_2O) on the Fe/SiO_2 ratio (w/w) of the molten slag at silica saturation; the trend lines show the average values of the data in each slag type

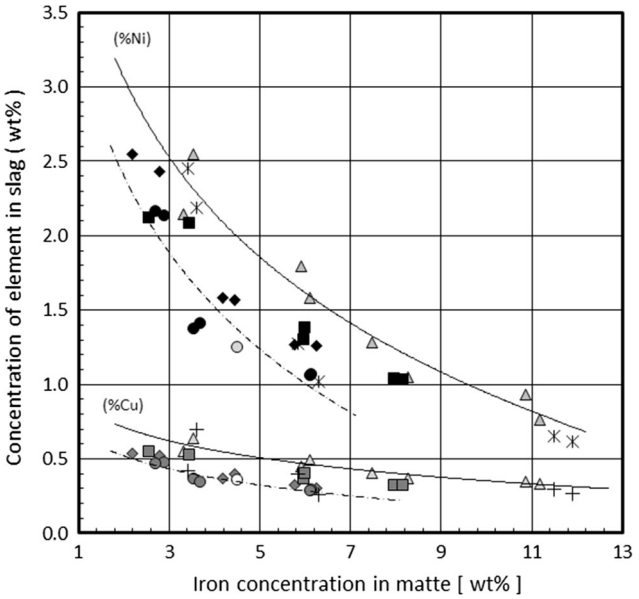

Fig. 6 Equilibrium concentrations of nickel and copper in the slag at 1673 K (1400 °C) as a function of iron concentration in matte at pSO2 = 0.1 atm; the symbols indicate the slag type: triangle—iron silicate, diamond—MgO-containing, square—K_2O-containing, circle—MgO & K_2O-containing and solid lines refer to metal concentrations in iron silicate slag, while dash-dotted lines to them in MgO & K_2O-containing slags; * and + are Ni and Cu data from MgO-free slags by Piskunen et al.,[17] and o as well as filled circle are Cu and Ni data by Font et al.[12] at MgO saturation

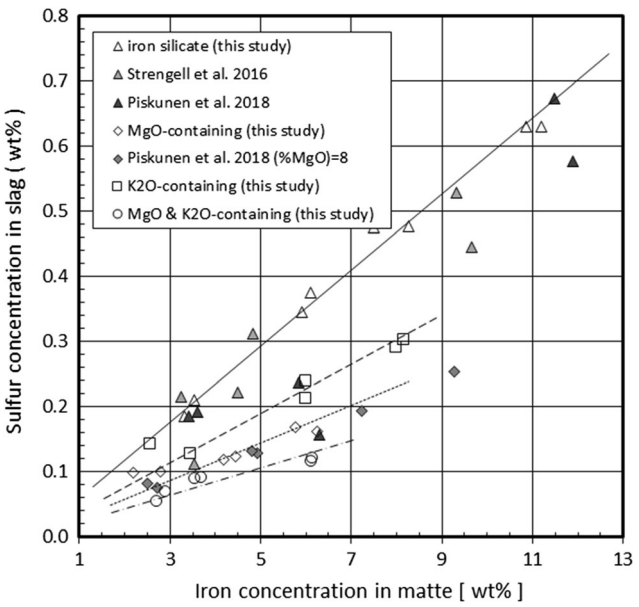

Fig. 7 Sulfur concentrations in the slags at silica saturation as a function of iron concentration in matte. The lines represent linear trend lines calculated according to the present observations

containing slags was significantly lower than in pure iron silicate slags in the experimental conditions investigated. Figure 7 reveals the linear dependences between the sulfur concentration in the slags and iron concentration in the sulfide matte within the experimental range of 2 to 11 wt.% Fe. The trend lines were drawn to cross zero solubility in iron-free mattes. This was based on the assumption of sulfur solubility by FeS species at the experimental oxygen partial pressures of this study.[25,26]

The concentrations of sulfur in pure iron silicate slag and in the MgO-containing slag obtained in this study were in a good agreement with the previous measurements by Strengell et al.[16] and Piskunen et al.,[17] though the earlier studies equilibrated the slags with nickel-copper-iron mattes with the Ni/Cu ratios of 2 and 4 (w/w), respectively. This indicates an insignificant effect of the Ni/Cu ratio on the activity of iron in the matte which is in good agreement with the findings by Font et al.[11,12] It complies with the almost ideal behavior of Cu_2S-FeS-Ni_3S_2 mattes.[26,27] On the other hand, the solubility of copper in slags measured by Strengell et al.[16] was slightly higher compared to the present observations, obviously due to the much higher copper concentration of matte in their study. Meanwhile, the solubility of nickel in their study was just slightly lower due to the same reason, related to differences in the matte compositions.

3.3 The MgO-SiO_2-FeO_X System

Addition of magnesia to iron silicate slags increases the liquidus temperature significantly already at small concentrations. At 1673 K (1400 °C) in the FeO-Fe_2O_3-SiO_2 system with 10 wt.% MgO, the homogeneous liquid slag domain is divided into two fields at different oxygen partial pressure ranges, i.e. a silica-saturated liquid and an olivine-saturated liquid, depending on their Fe/SiO_2 ratios.[17] The reason for this is the high stability of magnesium olivine, a silicate solid solution phase written in iron silicate slags as $(Fe, Mg)_2SiO_4$, which has also a high melting point.[28]

Figure 8 shows a quasibinary section of the Fe-O-MgO-SiO_2 system at constant oxygen partial pressure of 0.01 Pa ($10^{-7.0}$ atm) and fixed Fe/SiO_2 ratio of 2.0 (w/w) over the MgO range of w(MgO) = 0 to 0.20.

The diagram indicates that in the present constrained case, the lowest liquidus temperature in this section is about 1518 K (1245 °C) and at 1673 K (1400 °C) the slag becomes saturated with solid olivine when its magnesia concentration is about 9 wt.%. The solidus temperature is also relatively high and close to the liquidus, meaning that its viscosity below liquidus temperatures is strongly dependent on temperature,[30] due to rapid accumulation of solids when temperature is lowered. These fundamental limitations of the MgO-bearing iron silicate slags confirm a much narrower operational window, in particular for slags containing >5 wt.% MgO, compared to pure ternary iron silicate slags. The significant impact on potassia on the

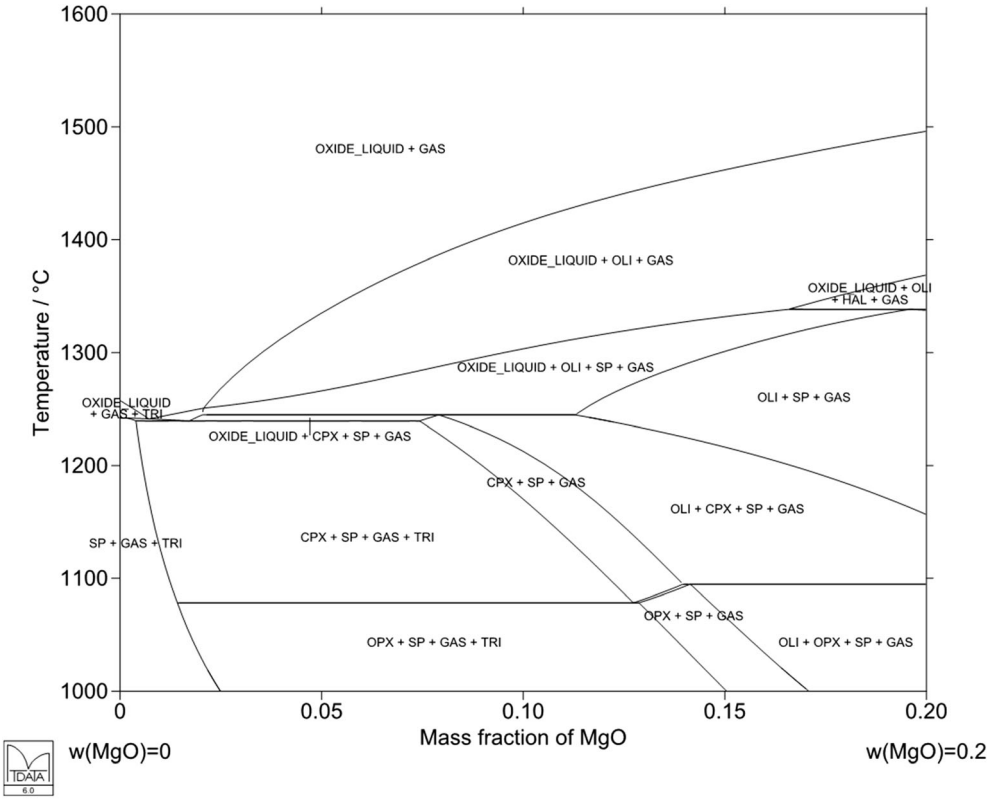
1600
1500
1400
1300
1200
1100
1000
Temperature / °C
OXIDE_LIQUID + GAS
OXIDE_LIQUID + OLI + GAS
OXIDE_LIQUID + OLI + HAL + GAS
OXIDE_LIQUID + OLI + SP + GAS
OLI + SP + GAS
OXIDE_LIQUID + GAS + TRI
OXIDE_LIQUID + CPX + SP + GAS
CPX + SP + GAS
OLI + CPX + SP + GAS
SP + GAS + TRI
CPX + SP + GAS + TRI
OPX + SP + GAS
OPX + SP + GAS + TRI
OLI + OPX + SP + GAS
0
0.05
0.10
0.15
0.20
Mass fraction of MgO
w(MgO)=0
w(MgO)=0.2

(a)

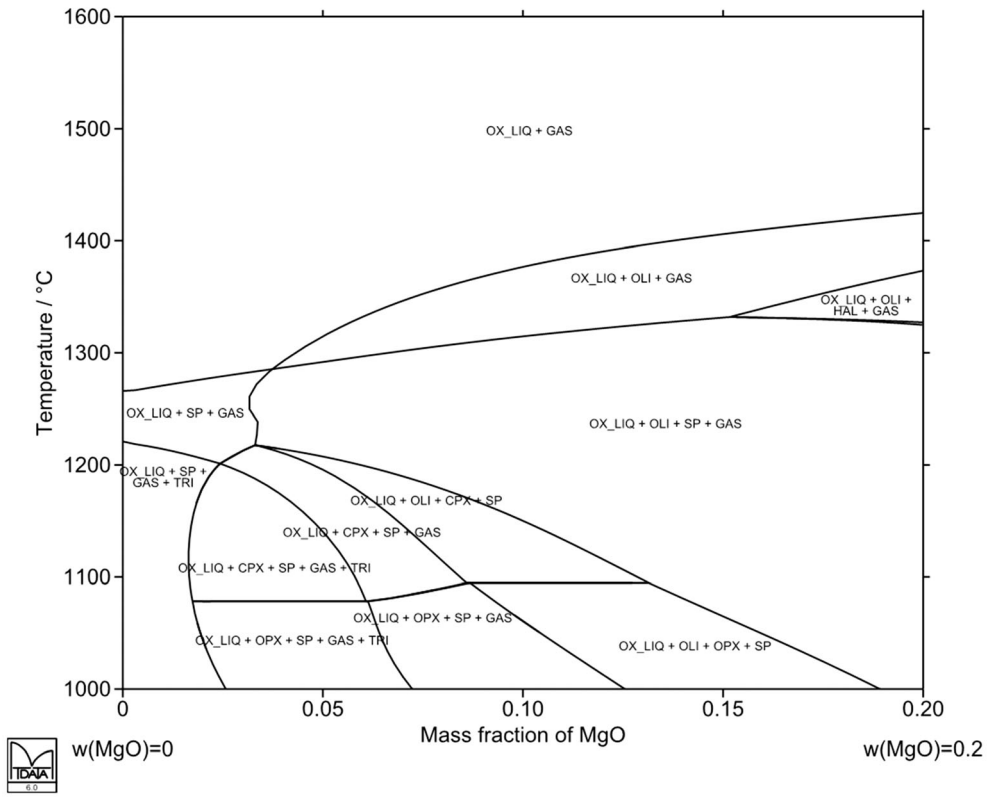
1600
1500
1400
1300
1200
1100
1000
Temperature / °C
OX_LIQ + GAS
OX_LIQ + OLI + GAS
OX_LIQ + OLI + HAL + GAS
OX_LIQ + SP + GAS
OX_LIQ + OLI + SP + GAS
OX_LIQ + SP + GAS + TRI
OX_LIQ + OLI + CPX + SP
OX_LIQ + CPX + SP + GAS
OX_LIQ + CPX + SP + GAS + TRI
OX_LIQ + OPX + SP + GAS
OX_LIQ + OPX + SP + GAS + TRI
OX_LIQ + OLI + OPX + SP
0
0.05
0.10
0.15
0.20
Mass fraction of MgO
w(MgO)=0
w(MgO)=0.2

(b)

◀**Fig. 8** An isopleth of the system Fe-O-MgO-SiO_2 under the constraints: (a) Fe/SiO_2 = 2.0 and pO2 = 10–7 atm, and (b) that with $w(K_2O)$ = 0.02 calculated with MTDATA using Mtox database[29]; the phase field labels refer to following minerals: CPX = clinopyroxene, HAL = wüstite (halite), OXDE_LIQUID = slag, OPX = orthopyroxene, SP = magnetite (spinel), TRI = tridymite

liquidus temperatures and phase equilibria is evident when comparing Fig. 8(a) and (b).

As a basic oxide, the presence of magnesia and potassia in the slag improves the metals distributions shifting their equilibria in the matte-slag systems to the sulfide phase, thus increasing their recoveries in the matte smelting and converting.[17,18]

3.4 The FeO_X-MgO-K_2O-SiO_2 System

Addition of potassium oxide in iron silicate slag decreases the liquidus temperature, increasing at the same time strongly its area of the molten phase domain when silica solubility is clearly increased by small K_2O additions, see Fig. 9. The additions of a few weight per cent in the slag cause an increase of several wt.% SiO_2 in the silica saturation line. Contrary to the other basic oxides, K_2O destabilizes the ferric ions in iron silicate slags.[31]

The experimental points shown on the diagram in Fig. 9 are the averages of the present observations at each slag composition. They are in fair agreement with the computational phase boundary reproduced by Mtox database of MTDATA,[29] except the slightly too strong effect of K_2O on the silica solubility. The liquid phase domain at $w(K_2O)$ = 0.00 has been painted grey. The experimental phase boundary data of Fig. 9, from six independent measurements each, have been collected numerically in Table 4.

4 Conclusions and Summary

The present study provides new fundamental phase equilibrium data regarding the slag chemistry in the DON smelting conditions, acquired in the equilibration experiments at 1673 K (1400 °C) and 0.1 atm p_{SO2} as a function

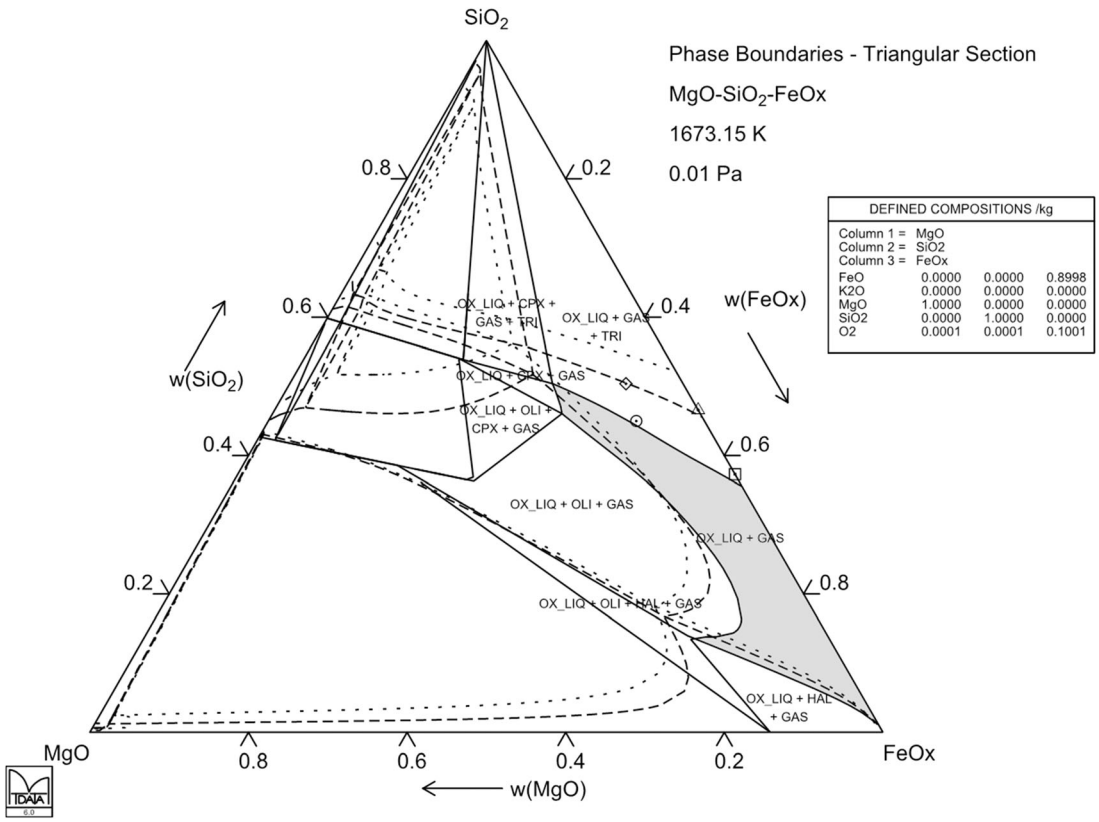

Fig. 9 A quasiternary section of system K_2O-FeO_X-MgO-SiO_2 at 1673 K (1400 °C) and $10^{-7.0}$ atm oxygen partial pressure with 0 (line), 1 (dashed line) and 2 wt.% K_2O (dotted line); CPX = clinopyroxene, HAL = wüstite, OLI = olivine and TRI = tridymite; the thermodynamic data from Mtox database[29]

Table 4 Experimental phase boundary data obtained at 1673 ± 3 K (1400 °C)

w(SiO_2)	w(MgO)	w(K_2O)	$\log_{10}p(O_2)$, atm
37.3 ± 0.3	0.0	0.0	−7.0 ± 0.1
45.0 ± 0.8	8.6 ± 0.3	0.0	−7.0 ± 0.1
46.6 ± 0.9	0.0	1.9 ± 0.2	−7.0 ± 0.1
50.4 ± 1.1	7.2 ± 0.3	1.5 ± 0.1	−7.0 ± 0.1

of iron concentration in matte, controlled by fixing p_{O2} (and consequently p_{S2}) in the system. In the present experimental conditions, a constrained case of slag compositions was investigated when the system was silica saturated. The particular focus of this study was on the nickel sulfide mattes containing less than 10 wt.% Fe, and representing the direct, high-grade matte smelting conditions with copper-lean feed mixtures of Ni/Cu = 5.2 (w/w).

The effects of the basic oxides investigated, MgO and K_2O, are interesting from the industrial viewpoint when processing sulfidic nickel bulk concentrates with a high MgO content. Correlations between the extent of iron oxidation or equilibrium oxygen partial pressure in the system and sulfidic matte composition as well as the solubilities of nickel and copper in slag were determined. Influence of magnesium and potassium oxides on the slag composition at silica saturation, i.e. solubilities of silica, nickel and copper in the slag, were investigated and proved significant even at the studied concentration levels of 1.9 wt.% K_2O and 8.6 wt.% MgO added separately in the slag. Their combined effect was even more pronounced with 1.5 wt.% K_2O and 7.2 wt.% MgO in the slag.

The primary phase boundaries of the molten slag were not strongly correlated with the prevailing oxygen pressure in the studied iron concentration range of the nickel sulfide matte. The chemical solubilities of copper and nickel in slag, however, were strongly increased when the oxidation degree of the system increased. Nickel concentration in the slag was essentially doubled when iron concentration in matte was decreased from 6 wt.% [Ni] to 2 wt.%, and for copper the losses in the same iron concentration range were increased by half. The current observations are in good agreement with the earlier data by Strengell et al.[16] and Piskunen et al.[17]

Acknowledgments Open access funding provided by Aalto University. The authors are indebted to EIT-RM Knowledge and Innovation Community (KIC), Boliden Harjavalta (Finland), and Eramet (France) for the financial support of this study (Grant # EIT/RAW MATERIALS/SGA2017/1). The EPMA measurements were carried out at Finnish Geological Survey (GTK) by Mr Lassi Pakkanen. This study utilized the Academy of Finland's RawMatTERS Finland Infrastructure (RAMI) based at Aalto University, GTK and VTT.

References

1. T. Mäkinen and P. Taskinen, State of the Art in Nickel Smelting: Direct Outokumpu Nickel Technology, *Miner. Process. Extract. Metall.*, 2008, **117**(2), p 86-94
2. P. Taskinen, K. Avarmaa, H. Johto, and P. Latostenmaa, Fundamental Process Equilibria of Base and Trace Elements in the DON Smelting of Various Nickel Concentrates, *Proceedings of the Extraction 2018. The Minerals, Metals & Materials Series*, B. Davis, M. Moats, and S. Wang, Ed., Springer, Cham, 2018, p 313-324
3. G. Mudd and S. Jowitt, A Detailed Assessment of Global Nickel Resource Trends and Endowments, *Econ. Geol.*, 2014, **109**(7), p 1813-1841
4. S. Jyrkönen, K. Haavanlammi, M. Luomala, J. Karonen, P. Suikkanen, Processing of PGM Containing Ni/Cu Bulk Concentrates in a Sustainable Way by Outotec Direct Nickel Flash Smelting Process, *Proceedings of the Ni-Co 2013*, T. Battle, M. Moats et al., Ed., Springer, Cham, 2013, p 325-334
5. T. Mäkinen and T. Ahokainen, 50 Years of Nickel Flash Smelting—Still Going Strong, *Pyrometallurgy of Nickel and Cobalt 2009*, J. Liu, J. Peacey, M. Barati, S. Kashani-Nejad, and B. Davis, Ed., CIM-MetSoc, Montreal, 2009, p 209-220
6. H. Johto, P. Latostenmaa, E. Peuraniemi, and K. Osara, Review of Boliden Harjavalta Nickel Smelter, *Proceedings of the Extraction 2018. The Minerals, Metals & Materials Series*, B. Davis, M. Moats, and S. Wang, Ed., Springer, Cham, 2018, p 81-87
7. I. Kojo, T. Mäkinen, and P. Hanniala, Direct Outokumpu Nickel Flash Smelting Process (DON)—High Metal Recoveries with Minimum Emissions, *Proceedings of the Nickel-Cobalt'97*, Vol III, C. Diaz, I. Holubec, and C. Tan, Ed., CIM-MetSoc, Montreal, 1997, p 25-34
8. T. Mäkinen and P. Taskinen, Physical Chemistry of Direct Nickel Matte Smelting, *Sulfide Smelting´98*, J. Asteljoki and R. Stephens, Ed., TMS, Warrendale (PA), 1998, p 59-68
9. H. Kellogg, Thermochemistry of Nickel Matte Converting, *Can. Metall. Q*, 1987, **26**(4), p 285-298
10. J. Font, Y. Takeda, and K. Itagaki, Phase Equilibrium Between Iron-Silicate Based Slag and Nickel-Iron Matte at 1573 K Under High Partial Pressures of SO_2, *Mater. Trans. JIM*, 1998, **39**(6), p 652-657
11. J. Font, M. Hino, and K. Itagaki, Phase Equilibrium and Minor Element Distribution Between Iron-Silicate Based Slag and Nickel-Copper-Iron Matte at 1573 K Under High Partial Pressures of SO_2, *Mater. Trans. JIM*, 1999, **40**(1), p 20-26
12. J. Font, M. Hino, and K. Itagaki, Phase Equilibrium Between FeO_x-SiO_2 Base Slags and Cu_2S-Ni_3S_2-FeS Mattes with Different Cu and Ni Contents at 1573 K, *Shigen-to-Sozai*, 1999, **115**(6), p 460-465 (in Japanese)
13. H. Henao, M. Hino, and K. Itagaki, Phase Equilibrium Between Ni-S Melt and FeO_x-SiO_2 or FeO_x-CaO Based Slag Under Controlled Partial Pressures, *Mater Trans*, 2002, **43**(9), p 2219-2222

14. H. Henao, M. Hino, and K. Itagaki, Solubility of Nickel in Slags Equilibrated with Ni-S Melt, *High Temp. Mater. Process.*, 2003, **22**(3–4), p 187-195
15. P. Taskinen, K. Seppälä, J. Laulumaa, and J. Poijärvi, Oxygen Pressure in the Outokumpu Flash Smelting Furnace—Part 2: The DON Process, *Miner. Process. Extract. Metall.*, 2001, **110**(2), p 101-108
16. D. Strengell, K. Avarmaa, H. Johto, and P. Taskinen, Distribution Equilibria and Slag Chemistry of DON Smelting, *Can. Metall. Q*, 2016, **55**(2), p 234-242
17. P. Piskunen, K. Avarmaa, H. O'Brien, L. Klemettinen, H. Johto, and P. Taskinen, Precious Metal Distributions in Direct Nickel Matte Smelting with Low-Cu Mattes, *Metall. Mater. Trans. B*, 2018, **49B**(1), p 98-112
18. D. Sukhomlinov, L. Klemettinen, O. Virtanen, Y. Lahaye, P. Latostenmaa, A. Jokilaakso, and P. Taskinen, Trace Element Distribution between Matte and Slag in DON Smelting. *Can. Metall. Q*. 2019 (under review)
19. N. Hellstén, P. Taskinen, H. Johto, and A. Jokilaakso, Trace Metal Distributions in Nickel Slag Cleaning, *Proceedings of the Extraction 2018. The Minerals, Metals & Materials Series*, B. Davis, M. Moats, and S. Wang, Ed., Springer, Cham, 2018, p 379-389
20. N. Hellstén, P. Taskinen, and A. Jokilaakso, Novel Method to Study Volatile Trace Elements in Electric Furnace Nickel Slag Cleaning, *Proceedings of the EMC 2019*, Vol 2, U. Waschki, Ed., GDMB, Clausthal-Zellerfeld, 2019, p 557-570
21. SGTE databases for MTDATA (http://resource.npl.co.uk/mtdata/databases.htm).
22. K. Avarmaa, H. Johto, and P. Taskinen, Distribution of Precious Metals (Ag, Au, Pd, Pt and Rh) Between Copper Matte and Iron Silicate Slag, *Metall. Mater. Trans. B*, 2016, **47B**(1), p 244-255
23. J. Pouchou and F. Pichoir, Basic Expression of "PAP" Computation for Quantitative EPMA, *Proceedings of the 11th International Congress on X-ray Optics and Microanalysis (ICXOM)*, J. Brown and R. Packwood, Ed., Publ. Univ. Western Ontario, Ontario, Canada, 1986, p 249-256
24. T. Ziebold, Precision and Sensitivity in Electron Probe Analysis, *Anal. Chem.*, 1967, **39**(8), p 858-861
25. N. Métrich, A. Berry, H. O'Neill, and J. Susini, The Oxidation State of Sulphur in Synthetic and Natural Glasses Determined by X-Ray Absorption Spectroscopy, *Geochim. Cosmochim. Acta*, 2009, **73**(8), p 2382-2399
26. D. Smythe, B. Wood, and E. Kiseeva, The S Content of Silicate Melts at Sulphide Saturation: New Experiments and a Model Incorporating the Effects of Sulphide Composition, *Am. Mineral.*, 2017, **102**(4), p 795-803
27. J. Koh and K. Itagaki, Measurements of Thermodynamic Quantities for Molten Ag_2S-Sb_2S_3 and Cu_2S-Ni_3S_2 Systems by Quantitative Thermodynamic Analysis, *Trans. JIM*, 1984, **25**(5), p 367-373
28. I. Jung, S. Decterov, and A. Pelton, Critical Thermodynamic Evaluation and Optimization of the FeO-Fe_2O_3-MgO-SiO_2 System, *Metall. Mater. Trans. B*, 2004, **35B**(5), p 877-889
29. J. Gisby, P. Taskinen, J. Pihlasalo, Z. Li, M. Tyrer, J. Pearce, K. Avarmaa, P. Björklund, H. Davies, M. Korpi, S. Martin, L. Pesonen, and J. Robinson, MTDATA and the Prediction of Phase Equilibria in Oxide Systems: 30 Years of Industrial Collaboration, *Metall. Mater. Trans. B*, 2017, **48B**(1), p 91-98
30. Ducret A., The Melting Point and Viscosity of Nickel Smelter Slags. PhD Thesis, University of Melbourne, Dept. Chemical Engineering, 1995
31. R. Tangeman, R. Lange, and L. Forman, Ferric-ferrous Equilibria in K_2O-FeO-Fe_2O_3-SiO_2 Melts, *Geochim. Cosmochim. Acta*, 2001, **65**(11), p 1809-1819